Journal of Luminescence 195 (2018) 176–180

Contents lists available at ScienceDirect

Journal of Luminescence

journal homepage: www.elsevier.com/locate/jlumin

Can measurement of the fluorescence lifetime of extracted blood PPIX predict atherosclerosis?

Letícia B. Sicchieri[a], Monica N. Da Silva[b], Ricardo E. Samad[a], Lilia C. Courrol[a,b,*]

[a] IPEN-CNEN/SP, São Paulo, SP, Brazil
[b] Departamento de Física, Univ. Federal de São Paulo, Diadema, SP, Brazil

ARTICLE INFO

Keywords:
Atherosclerosis
Protoporphyrin IX
Fluorescence lifetime
Blood analysis

ABSTRACT

In this work, fluorescence lifetime has been used to analyze protoporphyrin IX (PPIX) extracted from blood for diagnosing atherosclerosis. A total of 10 adult white male rabbits (New Zealand) were divided into the control group (CG), with a normal diet, and the experimental group (EG), subjected to a diet containing 1% cholesterol. Blood samples were collected from the animals, and protoporphyrin IX was extracted from the blood using acetone. The PPIX fluorescence lifetime (PPIXFL) was measured using time-correlated single photon counting, after excitation at 403 nm from a pulsed laser diode. It was found that the PPIX emission intensity was enhanced in the animals that had received a hypercholesterolemic diet. The CG and EG animal's fluorescence decays were fitted by three exponentials and the mean lifetimes were 4.0 ns and 9.5 ns, respectively. This lifetime dependence resulted in a calibration curve that allows the determination of the PPIX concentration with a temporal measurement. The obtained results show that fluorescence lifetime can potentially be used as a noninvasive, simple, rapid, and sensitive tool in atherosclerosis diagnosis.

1. Introduction

Atherosclerosis is characterized as a progressive disease in which the arterial wall thickens through a process of inflammation [1], oxidative stress [2] and flow restriction. The arterial plaques may also rupture leading to thrombosis and occlusion of the vessel, causing myocardial infarction, angina, ischemic stroke and some manifestations of peripheral arterial disease, such as acute limb ischemia [3].

The association between LDL (low density lipoprotein), HDL (high density lipoprotein) and total cholesterol levels with cardiovascular disease risk is well known [4]. However, the weak capacity to distinguish between patients who will and those who will not develop cardiovascular disease has prompted the search for further refinement of these traditional measures [5].

Existing screening and diagnostic methods are insufficient in identifying the disease before an event occurs. Diagnostic methods, including catheter-based techniques, can localize and characterize vulnerable plaques, but are invasive and require hospitalization [6].

Several optical spectroscopy techniques have previously been used in atherosclerosis characterization; these include fluorescence spectroscopy [7], optical coherence tomography, near-infrared absorption, Raman and diffuse reflectance spectroscopy [8–11].

Many authors have reported on the use of autofluorescence spectroscopy of tissues for distinguishing atherosclerotic plaques from normal tissue [12–14].

Time-Correlated Single Photon Counting (TCSPC) has usually been used to characterize biological tissue [15]. TCPSC generates decay curves by measuring single photons that are emitted from an excited fluorescent molecule, and creating a photon-intensity histogram [16,17]. The instrument registers the time between an excitation source pulse and the emitted photons, and after collecting a significant number of photons, a decay curve emerges from this data. The photon count is used because the emission intensity is directly proportional to the probability that a photon will be detected at a given time.

The lifetime of each fluorophore present in the tissue is highly sensitive to micro environmental changes. The decay dynamics are sensitive to intermolecular interactions and changes in the microenvironment, but are relatively independent of the artifacts existing in steady-state measurements. Several studies have shown that the techniques of time-resolved laser induced fluorescence [12] and fluorescence lifetime imaging microscopy [18] show potential for the characterization of the composition of atherosclerotic plaques, and to detect markers associated with plaque instability and rupture.

A potential marker for atherosclerosis in tissue and blood is protoporphyrin IX (PPIX). Spears et al. were the first to describe the accumulation of porphyrins in atheromatous lesions [19]. Peng et al.

* Corresponding author at: Departamento de Física, Univ. Federal de São Paulo, Diadema, SP, Brazil.
E-mail address: lccourrol@gmail.com (L.C. Courrol).

https://doi.org/10.1016/j.jlumin.2017.11.014
Received 3 November 2016; Received in revised form 4 May 2017; Accepted 12 November 2017
Available online 17 November 2017
0022-2313/ © 2017 Elsevier B.V. All rights reserved.

Table 1
Experimental Groups.

Groups	Number of Animals	Procedures
Control Group: CG	4	**Commercial diet washed with chloroform**
Experimental Group: EG	6	**Diet containing 1% cholesterol (Sigma Aldrich) diluted in chloroform**

previously detected PPIX in atheromatous plaques, after an intravenous administration of δ-aminolevulinic acid (ALA), in rabbits subjected to a hypercholesterolemic diet [20]. Silva et al. observed that PPIX that accumulates in atheromatous plaques transfers to the blood and can be analyzed by extracting porphyrin from total blood [21].

In the present study, we used the TCPSC technique to analyze blood PPIX for atherosclerosis diagnosis. Our work shows sufficient sensitivity and specificity to distinguish subjects with and without plaques, suggesting a new and noninvasive diagnostic method.

2. Materials and methods

2.1. Animal testing

A total of 10 adult white male rabbits (New Zealand species Orytolagus cuniculus, approximately 2.3 ± 0.1 kg, and ~3.5 months old) were divided into two experimental groups as shown in Table 1.

The animals were individually housed in a controlled environment that was maintained at 19 °C, and food and water were provided *ad libitum*. The Ethics Committee of UNIFESP approved the protocol of this study (Protocol no. 0374/12).

All 10 rabbits completed the experimental process. Ninety days after the start of the experiment, the animals were euthanized according to the American Veterinary Medical Association guidelines for euthanasia.

2.2. Porphyrin extraction

The animals' blood samples were collected 90 days from the start of the experiment. Three parts by volume of analytical grade acetone (P.A.-A.C.S. 790 g, 100% - SYNTH) were mixed with one part of the total blood collected. The mixture was centrifuged at 4000 rpm for 15 min. The clear supernatant of the mixture was stored in a clean tube and kept refrigerated, in the dark, until spectroscopic characterization was performed.

2.3. Fluorescence analyses

The emission spectra were obtained under excitation at 405 nm using a 1 mm optical path cuvette (Hellma). The sample fluorescence was measured from 550 to 750 nm using a Horiba Jobin Yvon Fluorolog 3 Fluorimeter.

The PPIX fluorescence lifetimes were obtained using a homemade system equipped with a pulsed diode laser (PDL 800-B, PicoQuant) that provides 45 ps pulses, centered at λ_{exc} = 403 nm, in an 8 MHz repetition rate pulse train. This yields a temporal instrument response function of, typically, (248 ± 1) ps FWHM, obtained by measuring the excitation light scattered by the cuvette. The average power was fixed at 0.1 mW. Detection was performed using a photomultiplier (Hamamatsu PMA 182-PM) and a RG610 longpass colored glass filter. A reflective ND filter ND30A (ThorLabs) was used to reduce the background noise. The obtained data was processed using PicoQuant PicoHarp 300 (TCSPC system connected to a PC through a USB 2.0 interface), and then analyzed using Mathematica 10.

The data are expressed as mean ± standard error of the mean (S.E.M.).

2.4. Artery excision and histological analysis

At the end of the experiment, the arteries were excised and washed with phosphate-buffered saline (PBS). Cryosections of the aortic arch specimens were cut in the vertical plane to a 10 μm thickness on a cryostat, and then mounted on glass slides and stained with Oil Red O (O0625 SIGMA-ALDRICH). Since lipids are soluble in the solvents used in standard histological tissue processing, fresh or fixed tissues were used for the cryostat sections. Oil-soluble dyes were used to stain and visualize the lipids in the sample sections, since the dyes have a greater solubility in the lipids than in their original solvents. Images were obtained using a Leica DMI6000 CS fluorescence microscope, a Leica DFC450FX digital video camera and Leica AF6000 software.

2.5. PPIX lifetime calibration curve

Protoporphyrin IX (Sigma CAS Number 553-12) was dissolved in acetone P.A. (Synth) and solutions containing concentrations ranging from 0 to 100 μg/L were prepared. Fluorescence lifetimes were obtained by the system already described.

3. Results and discussion

It was observed that within the 90-days duration of the experiment, atherosclerotic plaques were deposited in the arteries of rabbits fed the experimental diet containing 1% cholesterol. The images obtained from aortas stained with Oil Red are shown in Fig. 1, indicating a type IV, in

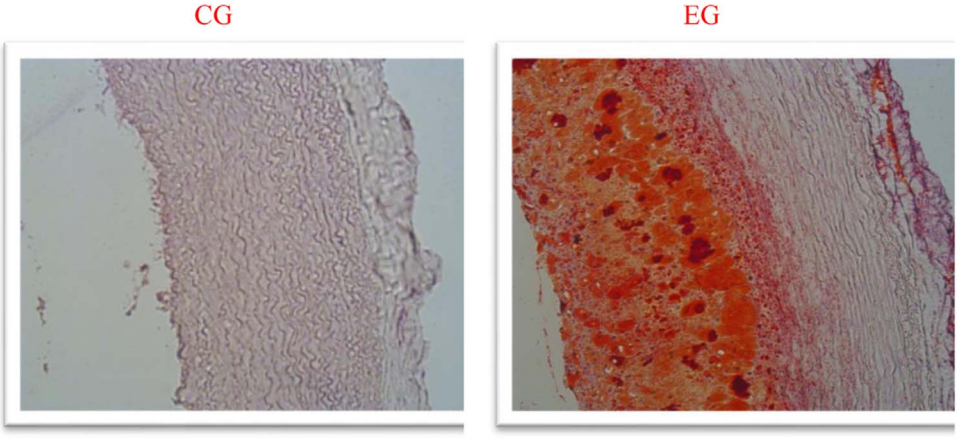

Fig. 1. Cross section of thoracic aortas from the control group (CG) and experimental group (EG) stained with Oil Red, indicating a type IV atherosclerotic plaque.

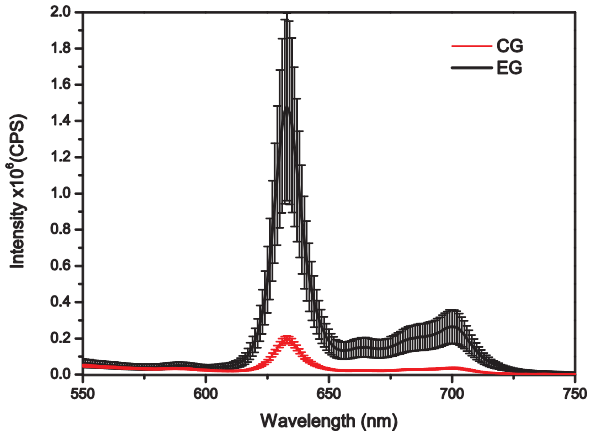

Fig. 2. Differences observed in the fluorescence signal of PPIX extracted from the blood of animals in the CG and EG groups. The curves represent an average of four spectra for the CG group and six spectra for the EG group.

a scale that runs up to VI, atheroma lesion. For the experimental group rabbits (high cholesterol diet), the intima layer was thickened and a considerable foamy cell infiltration and extracellular lipid accumulation was present. The aortas of the control group rabbits (fed a regular diet) had a normal thickness, and no lipid was present in the intima layer.

3.1. Blood fluorescence spectra

PPIX was extracted from the blood of the animals and emission spectra were obtained using excitation at 405 nm. Fig. 2 shows the resulting averaged spectra with two fluorescence bands, at 635 and 700 nm. The averaged PPIX emission intensity of the experimental group is higher than that of the control group. The mean ± SEM are significantly different between the two groups ($p < 0.05$).

The results shown in Fig. 2 indicate that porphyrin has accumulated in the blood of the experimental group animals. Previous studies have indicated that several types of porphyrins, including PPIX, accumulate in significant amounts in rapidly growing tissues such as atheromatous plaques [20,22]. The increase in blood PPIX emission follows the same trend as the growth of the plaques [7].

PPIX interacts with atherosclerotic plaques via low-density lipoprotein (LDL) receptors [21] in acidic environments [22]. In atherosclerotic lesions, the oxidized form of LDL, an important carrier of cholesterol, is uptaken by macrophages that accumulate progressively in the expanding arterial wall during the inflammatory response that drives atherogenesis. It is hypothesized that elevated PPIX accumulation in atherosclerotic tissues is due to higher concentration of LDL receptors compared to normal tissue. Actually, Guo et al. [20] showed that PPIX fluorescence was observed in macrophages. The ruptured erythrocytes release greater amounts of PPIX into the hyperlipidemic blood, resulting in an observed increase in the emission signal [23].

Several factors can explain the increase in the emission signal of PPIX extracted from the blood of animals with atherosclerotic plaques.

3.2. Blood fluorescence decay

The fluorescence decays of PPIX extracted from the blood of animals in the CG and EG groups using acetone were studied using excitation at 403 nm. Fig. 3 shows the normalized intensity fluorescence decay curves obtained. The time $t = 0$ is the moment at which the laser pulse finishes. All normalized intensity emission profiles, $I(t)$, were fitted by a triple-exponential decay curve:

$$I(t) = bg + A_1 \exp\left(-\frac{t}{\tau_1}\right) + A_2 \exp\left(-\frac{t}{\tau_2}\right) + A_3 \exp\left(-\frac{t}{\tau_3}\right) \quad (1)$$

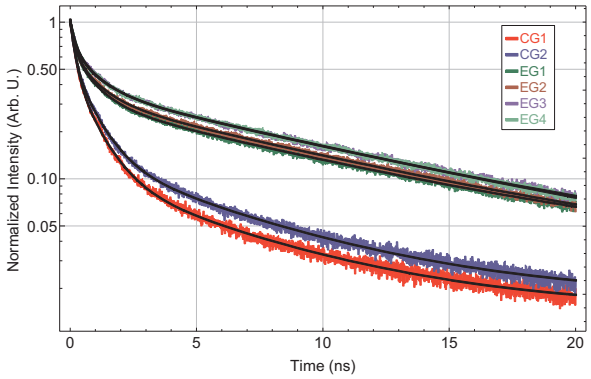

Fig. 3. Emission curves for the Control (CG) and Experimental (EG) groups, fitted by triple-exponential decay functions. The dashed curve, SR, is the measurement system response function.

where bg is the background noise, and the τ_i and A_i are the components lifetimes and their relative weights (amplitudes), respectively.

The quality of the fit was judged by the reduced-χ^2 value and inspection of the residuals distribution. The amplitude-weighted lifetime $< \tau >$ was calculated according to:

$$<\tau> = \frac{\sum A_i \tau_i^2}{\sum A_i \tau_i} \quad (2)$$

Observing Fig. 3 and Table 2 is clear that the EG animals exhibit longer weighted lifetime emissions by a factor over two, providing a parameter to quantify the PPIX concentration on the blood. All samples exhibited a short lifetime, around 0.2 ns, attributed to the acetone, a decay time around 1 ns attributed to other proteins in the blood that contribute with additional decay processes (not discussed here), and a longer decay time, rising from 6 to 11 ns with the increasing PPIX concentration. According to Brancaleon et al. [24], the fluorescence lifetime of PPIX depends on the solvent and the emission wavelength. Brancaleon's values for PPIX in acetone have a long lifetime around 12.0 ± 0.8 ns and a short lifetime at 1.4 ± 0.3 ns, in the spectral region between 650 and 680 nm.

3.3. PPIX calibration curve

The concentrations of the PPIX in each sample, were estimated from a PPIX calibration curve. For this study a commercial PPIX solution from Sigma was diluted in P.A. acetone, and emission decay profiles were obtained as a function of the PPIX concentration ranging from 0 (acetone) to 100 μg/L. The results are shown in Fig. 4a. Differently from the analysis adopted for the animal samples, the emission curves were fitted by double-exponential decays. This treatment was used because only two lifetimes were expected here, one for the acetone and other for the PPIX, differently from the animal samples solutions. The amplitude-weighted lifetimes, $< \tau >$, were also calculated according to Eq. (2), and are shown as a function of the PPIX concentration in Fig. 4b. The amplitude-weighted lifetimes increase as the PPIX concentration rises, until saturation is reached around 11 ns for ~ 30 μg/L. In the solutions with PPIX concentrations above 30 μg/L, the longer lifetime predominates; for lower concentrations, where both short and long lifetimes contribute, the weighted lifetimes show a strong dependence on the PPIX quantity, enabling the solution concentration to be determined from temporal measurements. These results agree with studies reported previously [25] that describe a lifetime around 11 ns for highly concentrated PPIX acetone solutions. The differences observed between low and high concentration PPIX decay profiles can be explained by the presence of aggregated forms of PPIX at higher concentrations [26], since monomeric PPIX is preferentially formed at low concentrations, while planar aggregates tend to form at higher concentrations.

A saturation curve for the weighted lifetime, given by:

Table 2
Amplitude-weighted lifetimes obtained from the fitting parameters for the control and experimental groups and components times (τ_i). The last line shows the mean lifetime for each group.

Animal	CG		EG	
	τ_i (ns)	$< \tau >$ (ns)	τ_i (ns)	$< \tau >$ (ns)
1	τ_1 = 0.199 ± 0.001 τ_2 = 6.02 ± 0.09 τ_3 = 0.91 ± 0.01	3.65 ± 0.07	τ_1 = 0.184 ± 0.002 τ_2 = 10.03 ± 0.08 τ_3 = 0.93 ± 0.01	8.93 ± 0.07
2	τ_1 = 0.175 ± 0.001 τ_2 = 6.22 ± 0.06 τ_3 = 0.88 ± 0.01	4.17 ± 0.05	τ_1 = 0.198 ± 0.002 τ_2 = 10.42 ± 0.08 τ_3 = 0.99 ± 0.01	9.39 ± 0.08
3			τ_1 = 0.185 ± 0.003 τ_2 = 10.62 ± 0.09 τ_3 = 0.98 ± 0.01	9.71 ± 0.09
4			τ_1 = 0.215 ± 0.003 τ_2 = 11.06 ± 0.09 τ_3 = 1.02 ± 0.01	10.17 ± 0.09
Mean lifetime		**3.96 ± 0.04**		**9.49 ± 0.04**

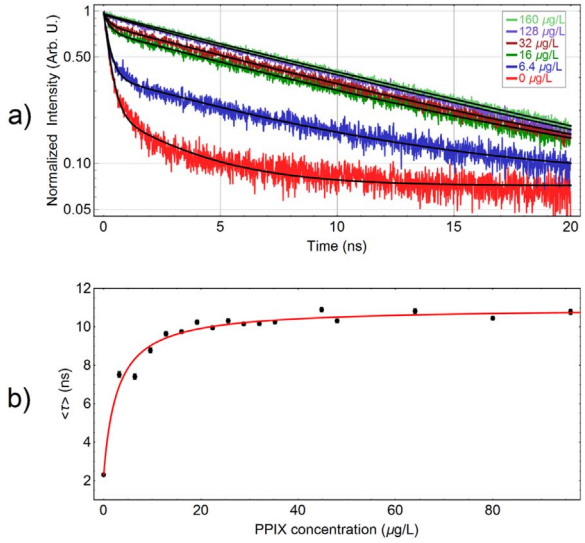

Fig. 4. a) Decay profiles of PPIX acetone solutions – only a few representative measured curves are shown to avoid cluttering – with fitted double exponentials (continuous black lines). The dashed curve, SR, is the measurement system response function. b) amplitude-weighted lifetimes, $< \tau >$, obtained for the curves shown in a) as a function of the PPIX concentration, along with a fitted saturation curve (continuous red line).

$$\tau(C) = \frac{aC}{1+bC} + \tau_0, \tag{3}$$

was fitted to the data, where τ_0 is the shortest lifetime and C is the PPIX concentration in μg/L, and the fit parameters are a = (3.07 ± 0.43) ns/(μg/L), b = (0.353 ± 0.52) L/μg and τ_0 = (2.31 ± 0.18) ns. To determine the PPIX concentration in an acetone solution from its measured weighted decay time, the inverse of Eq. (3) must be used with the fitted parameters:

$$C(\tau) = \frac{\tau - \tau_0}{a - b(\tau - \tau_0)} \tag{4}$$

From Eq. (4), the PPIX blood concentrations for CG and EG animals were found to be (0.66 ± 0.02) μg/L and (13.40 ± 0.33) μg/L, respectively.

Fluorescence lifetime is the time it takes for the number of excited PPIX molecules to decay to 1/e (36%) of the original population. Artifacts which are generated by diffused light propagation and by detection geometries do not affect fluorescence lifetime since this characteristic does not depend on the light path [27]. One of the major advantages of the fluorescence lifetime technique is the fact that it is independent of concentration. However, this is only true for a certain range of concentrations, in which fluorophores do not interact chemically or photonically [28]. At high concentrations, the fluorescence lifetime can increase due to a trivial process of photon re-absorption. In a re-absorption process, the fluorescence lifetime remains unchanged and only the measurable lifetime value is affected, often significantly. For example, in highly concentrated solution, the lifetime of Rhodamine 6G changes from ~ 4 ns to ~ 11 ns [29]. Similarly, DBPI increases from 3.7ns to 8.5 ns [30]. In the present study, PPIX exhibits a similar trend, with an exponential increase in fluorescence lifetime at high concentrations.

In the case of our work with PPIX, the fluorescence lifetime obtained for PPIX extracted from animals from the CG and EG groups, we observed a triple-exponential decay with averaged lifetime of 9.5 ns for EG, and 4 ns for CG.

Plasma extracted PPIXFL detection for diagnosis of atherosclerosis has several advantages. Firstly, PPIXFL is more specific for atherosclerosis than inflammatory or coagulation biomarkers [31]. Secondly, even though atherosclerotic plaque imaging can be a much more precise predictor of destabilization, its employment can be costly and is not as practical as the measurement of PPIX fluorescent lifetime. PPIXFL is simple, rapid, and economical.

Using a simple TCSPC fluorescence lifetime setup is possible to determine the PPIX concentration in the blood of animals, indicating the presence of atherosclerosis. This technique can potentially be extended for humans, presenting the advantages of being minimally invasive and faster than traditional ones to detect atherosclerotic plaques. These are great benefits for patients when compared to conventional plaque diagnosis methods that use contrast agents, and require hospitalization or specialized and expensive instrumentations and technicians, and take at least a few hours to deliver results. More studies and trials are needed before turning this technique into a clinical method.

4. Conclusions

The results obtained show that it is possible to differentiate the presence of atherosclerotic plaques by lifetime fluorescence analysis of PPIX extracted from the blood. We have shown that a weighted lifetime around 9.5 ns indicate the presence of a type IV atheroma lesion, opening the possibility of detecting earlier stages for shorter weighted lifetimes. The values found for animals with normal arteries are approximately 4 ns.

By an obtained PPIX calibration curve it was possible to determine the PPIX blood concentrations. The values found were (0.66 ± 0.02) μg/L and (13.40 ± 0.33) μg/L for CG and EG animals, respectively.

For humans, larger individual variation is expected for non-atherosclerotic samples, thereby reducing the diagnostic accuracy of PPIX

fluorescence and affecting its use as a screening tool. Nevertheless, PPIXFL should be a useful biomarker tool for diagnosing initial atheromatous plaque formation.

Acknowledgments

This work was supported by the Fundação de Amparo a Pesquisa do Estado de São Paulo (FAPESP), Grant no. 2014/06960-9.

References

[1] R. Ross, Mechanisms of disease - atherosclerosis - an inflammatory disease, New Engl. J. Med. 340 (1999) 115–126.
[2] G.M. Chisolm, D. Steinberg, The oxidative modification hypothesis of atherogenesis: an overview, Free Radic. Biol. Med. 28 (2000) 1815–1826.
[3] J.S. Ross, N.E. Stagliano, M.J. Donovan, R.E. Breitbart, G.S. Ginsburg, Atherosclerosis and cancer - common molecular pathways of disease development and progression, Atherosclerosis Vi 947 (2001) 271–293.
[4] W.P. Castelli, Lipids, risk factors and ischaemic heart disease, Atherosclerosis 124 (1996) S1–S9.
[5] E. Di Angelantonio, P. Gao, L. Pennells, S. Kaptoge, M. Caslake, A. Thompson, A.S. Butterworth, N. Sarwar, D. Wormser, D. Saleheen, C.M. Ballantyne, B.M. Psaty, J. Sundstrom, P.M. Ridker, D. Nagel, R.F. Gillum, I. Ford, P. Ducimetiere, S. Kiechl, R.P.F. Dullaart, G. Assmann, R.B. D'Agostino, G.R. Dagenais, J.A. Cooper, D. Kromhout, A. Onat, R.W. Tipping, A. Gomez-de-la-Camara, A. Rosengren, S.E. Sutherland, J. Gallacher, F.G.R. Fowkes, E. Casiglia, A. Hofman, V. Salomaa, E. Barrett-Connor, R. Clarke, E. Brunner, J.W. Jukema, L.A. Simons, M. Sandhu, N.J. Wareham, K.-T. Khaw, J. Kauhanen, J.T. Salonen, W.J. Howard, B.G. Nordestgaard, A.M. Wood, S.G. Thompson, S.M. Boekholdt, N. Sattar, C. Packard, V. Gudnason, J. Danesh, C. Emerging Risk Factors, Lipid-related markers and cardiovascular disease prediction, JAMA-J. Am. Med. Assoc. 307 (2012) 2499–2506.
[6] B.D. MacNeill, H.C. Lowe, M. Takano, V. Fuster, I.K. Jang, Intravascular modalities for detection of vulnerable plaque - current status, Arterioscler. Thromb. Vasc. Biol. 23 (2003) 1333–1342.
[7] M. Nascimento da Silva, L.B. Sicchieri, F. Rodrigues de Oliveira Silva, M.F. Andrade, L.C. Courrol, Liquid biopsy of atherosclerosis using protoporphyrin IX as a biomarker, Analyst 139 (2014) 1383–1388.
[8] P.R. Moreno, J.E. Muller, Identification of high-risk atherosclerotic plaques: a survey of spectroscopic methods, Curr. Opin. Cardiol. 17 (2002) 638–647.
[9] Z.A. Fayad, V. Fuster, Clinical imaging of the high-risk or vulnerable atherosclerotic plaque, Circ. Res. 89 (2001) 305–316.
[10] G. Pasterkamp, E. Falk, H. Woutman, C. Borst, Techniques characterizing the coronary atherosclerotic plaque: influence on clinical decision making, J. Am. Coll. Cardiol. 36 (2000) 13–21.
[11] L. Marcu, Fluorescence lifetime in cardiovascular diagnostics, J. Biomed. Opt. 15 (2010).
[12] L. Marcu, Q.Y. Fang, J.A. Jo, T. Papaioannou, A. Dorafshar, T. Reil, J.H. Qiao, J.D. Baker, J.A. Freischlag, M.C. Fishbein, In vivo detection of macrophages in a rabbit atherosclerotic model by time-resolved laser-induced fluorescence spectroscopy, Atherosclerosis 181 (2005) 295–303.
[13] L. Marcu, M.C. Fishbein, J.M.I. Maarek, W.S. Grundfest, Discrimination of human coronary artery atherosclerotic lipid-rich lesions by time-resolved laser-induced fluorescence spectroscopy, Arterioscler. Thromb. Vasc. Biol. 21 (2001) 1244–1250.
[14] J.M.I. Maarek, L. Marcu, W.J. Snyder, W.S. Grundfest, Time-resolved fluorescence spectra of arterial fluorescent compounds: reconstruction with the laguerre expansion technique, Photochem. Photobiol. 71 (2000) 178–187.
[15] W. Becker, A. Bergmann, C. Biskup, Multispectral fluorescence lifetime imaging by TCSPC, Microsc. Res. Tech. 70 (2007) 403–409.
[16] C. Albrecht, Joseph, R. Lakowicz, Principles of Fluorescence Spectroscopy, 3rd edition, Berlin/Heidelberg, 2008, pp. 1223–1224.
[17] E. Terpetschnig, H. Szmacinski, A. Ozinskas, J.R. Lakowicz, Synthesis of Squaraine-n-hydroxysuccinimide esters and their biological application as long-wavelength fluorescent labels, Anal. Biochem. 217 (1994) 197–204.
[18] D.S. Elson, J.A. Jo, L. Marcu, Miniaturized side-viewing imaging probe for fluorescence lifetime imaging (FLIM): validation with fluorescence dyes, tissue structural proteins and tissue specimens, New J. Phys. 9 (2007).
[19] J.R. Spears, J. Serur, D. Shropshire, S. Paulin, Fluorescence of experimental atheromatous plaques with hematoporphyrin derivative, J. Clin. Investig. 71 (1983) 395–399.
[20] C.H. Peng, Y.S. Li, H.J. Liang, J.L. Cheng, Q.S. Li, X. Sun, Z.T. Li, F.P. Wang, Y.Y. Guo, Z. Tian, L.M. Yang, Y. Tian, Z.G. Zhang, W.W. Cao, Detection and photodynamic therapy of inflamed atherosclerotic plaques in the carotid artery of rabbits, J. Photochem. Photobiol. B-Biol. 102 (2011) 26–31.
[21] M.N. da Silva, L.B. Sicchieri, F.R.D. Silva, M.F. Andrade, L.C. Courrol, Liquid biopsy of atherosclerosis using protoporphyrin IX as a biomarker, Analyst 139 (2014) 1383–1388.
[22] S.Y. Guo, X. Sun, J.L. Cheng, H.B. Xu, J.H. Dan, J. Shen, Q. Zhou, Y. Zhang, L.L. Meng, W.W. Cao, Y. Tian, Apoptosis of THP-1 macrophages induced by protoporphyrin IX-mediated sonodynamic therapy, Int. J. Nanomed. 8 (2013) 2239–2246.
[23] G. Camejo, C. Halberg, A. Manschik-Lundin, E. Hurt-Camejo, B. Rosengren, H. Olsson, G.I. Hansson, G.B. Forsberg, B. Ylhen, Hemin binding and oxidation of lipoproteins in serum: mechanisms and effect on the interaction of LDL with human macrophages, J. Lipid Res. 39 (1998) 755–766.
[24] L. Brancaleon, S.W. Magennis, I.D.W. Samuel, E. Namdas, A. Lesar, H. Moseley, Characterization of the photoproducts of protoporphyrin IX bound to human serum albumin and immunoglobulin G, Biophys. Chem. 109 (2004) 351–360.
[25] P. Natarajan, C. Raja, Novel features of the interpolymer self-organisation behaviour investigated using covalently linked protoporphyrin IX as fluorescent probe in the macromolecules, Eur. Polym. J. 37 (2001) 2207–2211.
[26] F. Ricchelli, S. Gobbo, G. Moreno, C. Salet, L. Brancaleon, A. Mazzini, Photophysical properties of porphyrin planar aggregates in liposomes, Eur. J. Biochem. 253 (1998) 760–765.
[27] Y. Shu-Chi Allison, S.P. Michael, E.H. Joseph, F. Qiyin, Time- resolved fluorescence in photodynamic therapy, Photonics 1 (2014) 530–564.
[28] M.Y. Berezin, S. Achilefu, Fluorescence lifetime measurements and biological imaging, Chem. Rev. 110 (2010) 2641–2684.
[29] K.A. Selanger, J. Falnes, T. Sikkeland, Fluorescence lifetime studies of rhodamine 6G in methanol, J. Phys. Chem. 81 (1977) 1960–1963.
[30] S.A. ElDaly, S. Hirayama, Re-absorption and excitation energy transfer of N,N'-bis (2,5-di-tert-butylphenyl)-3,4:, 10-perylenebis(dicarboximide) (DBPI) laser dye, J. Photochem. Photobiol. A-Chem. 110 (1997) 59–65.
[31] K. Kaikita, T. Ono, S. Iwashita, N. Nakayama, K. Sato, E. Horio, S. Nakamura, K. Tsujita, S. Tayama, S. Hokimoto, T. Sakamoto, K. Nakao, S. Oshima, S. Sugiyama, H. Ogawa, Impact of CYP2C19 polymorphism on platelet function tests and coagulation and inflammatory biomarkers in patients undergoing percutaneous coronary intervention, J. Atheroscler. Thromb. 21 (2014) 64–76.